water

MDPI

Article

Effective Removal of Reactive and Direct Dyes from Colored Wastewater Using Low-Cost Novel Bentonite Nanocomposites

Yusra Chauhdary [1], Muhammad Asif Hanif [1], Umer Rashid [2,*], Ijaz Ahmad Bhatti [1], Hafeez Anwar [3], Yasir Jamil [3], Fahad A. Alharthi [4] and Elham Ahmed Kazerooni [5]

1 Nano and Biomaterials Lab, Department of Chemistry, University of Agriculture, Faisalabad 38040, Pakistan
2 Institute of Nanoscience and Nanotechnology (ION2), Universiti Putra Malaysia, Serdang 43400, Selangor, Malaysia
3 Department of Physics, University of Agriculture, Faisalabad 38040, Pakistan
4 Chemistry Department, College of Science, King Saud University, Riyadh 1145, Saudi Arabia
5 Department of Applied Biosciences, Kyungpook National University, Daegu 41566, Korea
* Correspondence: umer.rashid@upm.edu.my or dr.umer.rashid@gmail.com; Tel.: +60-97697393

Abstract: The present study was aimed to remove direct violet-51, reactive green-5, reactive red, and acid red dyes by novel bentonite clay nanocomposites prepared using sodium metasilicate and potassium ferricyanide. The effect of temperature, pH, adsorbent amount, contact time, and initial concentration were studied to optimize the removal process. Various adsorption isotherms (Temkin, Freundlich isotherm, Langmuir isotherm, Harkin Jura, and Dubinin Radushkevich models) and kinetic models (pseudo-first order and pseudo-second order) were applied to adsorption data to find out the best fit model, i.e., Freundlich isotherm and pseudo-second order model. The prepared samples of bentonite nanocomposites were characterized using scanning electron microscopy (SEM) and Fourier transform infrared spectroscopy (FTIR). Bentonite treated with sodium metasilicate and potassium ferricyanide removed 96.6% of direct violet-51 dye, bentonite treated with sodium metasilicate removed 95%, bentonite treated with potassium ferricyanide removed 94%, and pure bentonite removed 80% of the dye from the solution.

Keywords: bentonite; sodium metasilicate; potassium ferricyanide; direct violet-51 dye

Citation: Chauhdary, Y.; Hanif, M.A.; Rashid, U.; Bhatti, I.A.; Anwar, H.; Jamil, Y.; Alharthi, F.A.; Kazerooni, E.A. Effective Removal of Reactive and Direct Dyes from Colored Wastewater Using Low-Cost Novel Bentonite Nanocomposites. *Water* **2022**, *14*, 3604. https://doi.org/10.3390/w14223604

Academic Editors: Vincenzo Naddeo and Chi-Wang Li

Received: 7 October 2022
Accepted: 4 November 2022
Published: 8 November 2022

1. Introduction

In developing countries, industrial wastewater management is one of the major issues under discussion. Untreated textile effluents are discharged in the drain which deteriorate the water bodies [1]. Almost 10 to 25% of the textile dyes are lost during the processing as effluents. Wastewater effluents are mostly organic in nature with dissolved oils and coloring agents. Moreover, fabric soaked with grease and oil adds to solid wastes that are hazardous and toxic to environment [2]. The release of toxic wastewater from industries is becoming a constant threat to the well-being of natural water resources and populations. Because of poor wastewater management policies of developing countries, 20% to 40% waterborne diseases are caused by industrial wastewater [3,4]. Seventy thousand tons of dyestuff is manufactured on annual basis, and the majority of these synthetic dyes are water soluble. These dyes have very complex structures, which make them less biodegradable that is why effective treatment methods are of interest currently [5–7].

A wide range of conventional methods have been investigated for dye removal extensively, but they have their own limitations, and these are not profitable at economical level. Principally, adsorption can be employed at large scale for the purification of wastewater at relatively large flow rates. Moreover, this method produces high-quality effluent that does not form harmful substances such as free radicals and ozone which are produced in photodegradation process via Ultraviolet (UV) radiation. The process of adsorption is fast,

universal, and inexpensive. Various nano conventional sorbents are employed for removing chemical pollutants like chitin, peat, sulfonated coal, wheat straw, organomon t-morillonite, apple pomace, fly ash, dyestuff, and coir pith [8]. There are specific interactions that occurs between the adsorbed contaminants and adsorbent materials. These interactions may be due to the simple mass transfer from liquid to solid phase. Three components are used in these complicated interactions i.e., adsorbate, adsorbent, and wastewater. Wastewater comprises synthetic solution and effluents. Typically, in a ternary system such as this, main interaction forces are the affinity between the adsorbate and adsorbent that control adsorption [9].

In modern-day technology, clay nanocomposites are considered more economical and effective adsorbent for textile wastewater treatment. Because of the economic benefits and easy availability, natural clay minerals are used intensively. However, unfortunately, they have limited potential for micro-pollutant removal, less surface area, and lack standard protocol for recovery and regeneration in aqueous system. Nanocomposite adsorbents provide an appropriate substitute to expensive and less efficient adsorbent material. Clay polymer nanocomposites are gaining researchers' attention day by day due to their remarkable characteristics regarding water decontamination [10]. Despite many other known nanocomposite adsorbents, bentonite is recognized as one of the most effective clays for the adsorption of dyes. Aluminum silicate minerals are the main component of bentonite clay, which are responsible for uniform pores, wide interlayers spacing, and non-swelling activities. Bentonite is an inert and ecofriendly material that has good thermal stability, which is why it is used extensively for catalysis. To increase its catalytic and adsorption performance, bentonite is modified by mixing with different metals and metal oxides. It is reported that Na^+ is present in the interlayers of bentonite, which increases the surface area and basal spacing [11].

Bentonite has been used in its original form by various researchers for the removal of dyes from colored wastewater. Previously, bentonite was used to remove commercial dye, Basic Red 2 (BR2), effectively from wastewater as it was found to have cation exchange capacity [12]. In another study by Khelifi and Ayari, [13], congo red dye was removed effectively using bentonite in batch experiments. Regeneration studies were also conducted successfully. Tahir and Rauf [14] utilized bentonite for malachite green removal from aqueous solutions under various conditions including adsorbate concentrations, temperature, pH, and shaking time were optimized during study. The dye removal process was found to be physical adsorption. Adsorption is a physical process that usually comes with several disadvantages, including the low surface area, high cost of adsorbent, and hard separation of the adsorbent from dye.

In this investigational study, economical and novel bentonite nanocomposites were employed to deteriorate dyestuff, which includes direct voilet-51, reactive green 5, reactive red, and acid red. The dye removal process was used to optimize contact time, initial concentration of dye, and effect of temperature. This study is the first report to check and compare kinetic and adsorption isotherms of natural and modified bentonite nanocomposites.

2. Materials and Methods

2.1. Dyes and Bentonite Nanocomposites

Reactive Green-5, Reactive Red, Direct violet-51, and Acid Red Dyes used in this research work were purchased from the local dye textile market of Faisalabad. For the determination of lambda max for four dyes, namely Reactive Green-5, Reactive Red, Direct violet-51, and Acid Red, 50 ppm solution was prepared by dissolving 5 mg of dyes into 100 mL of distilled water. All the dye solutions were then run through the 721 D UV-visible spectrophotometer (Wincom Company Ltd., Changsha, China). Each dye was scanned in the wavelength ranging from 380 nm to 1000 nm [15].

Bentonite clay was also purchased from a local market. Bentonite was ground into fine particles with the help of pestle and mortar and then passed though the sieve to

get uniform size powder. This fine bentonite powder was then used to prepare bentonite nanocomposites [16]. A simple procedure was used to prepare nanocomposites of bentonite. Five grams of Bentonite clay was mixed with each of potassium ferricyanide solution, sodium meta silicate solution, and with the mixture of both potassium ferricyanide and sodium meta silicate solution in a separate beaker to make a paste. The paste was allowed to stand for 24 h at room temperature and then washed thoroughly with distilled water until clear filtrate was obtained. All the solid residue was collected carefully from the filter paper. The paste-like material obtained after filtration were subjected to drying in the WHL-25A oven (Hino Teck, Tianjin, China) at 150 °C for one hour. Once the paste dried, it was ground into fine powder, and it was ready to use as adsorbent in the form of bentonite nanocomposites.

2.2. Adsorption Studies

The adsorption studies were performed in 15 mL capacity Falcon tubes containing 10 mL of dye solution (50 ppm) and 0.01 g of bentonite or bentonite nanocomposites using PA250/25H orbital shaker (NANBEI Instrument limited, Zhengzhou, China) at the speed of 300 rpm for 2 h [17]. Microfilters (Membrane Filter Products System, Malaysia) (0.45 µm) were used to filter the dye solution using a disposable plastic syringe. The absorbance of each solution was read before and after adsorption process using a UV-visible spectrophotometer (Wincom Company Ltd., Changsha, China) [18]. The concentration of dye solutions was determined using standard curves. The formula used for calculating the *standard factor* was:

$$Standard\ Factor = \frac{Concentration}{Absorbance} \quad (1)$$

The following formula was used to calculate the *%age removal* of dyes [19]:

$$\%age\ removal = \frac{C_o - C_e}{C_o} \times 100 \quad (2)$$

where C_o is the blank concentration, and C_e is the sample concentration.

To study the effect of initial dye concentration, the dye solutions of 5 ppm, 10 ppm, 15 ppm, 25 ppm, and 50 ppm were prepared from 100 ppm stock solution. The effect of various doses (i.e., 0.05 g, 0.1 g, 0.2 g, 0.3 g, and 0.4 g) of pure bentonite, bentonite treated with sodium metasilicate, bentonite treated with potassium ferricyanide, and bentonite treated with both sodium metasilicate and potassium ferricyanide was accessed at 50 ppm initial dye concentration. To check the effect of pH on the adsorption of dye (50 ppm) on adsorbent surface, the experiment was performed by varying the pH from 5 to 10 of dye solutions by using 0.1 N NaOH and 0.1 N HCl prior to adding adsorbents. At 50 ppm of dye solution concentration and 0.05 g of adsorbent dose optimization of time and temperature was done. Removal of dyes using different adsorbents at varying times of 15, 30, 60, 120, and 240 min was observed. The influence of temperature on adsorption was monitored at 30, 40, 50, 60, and 70 °C. The solutions were shaken in an orbital shaker for 2 h at 300 rpm shaking speed. While optimizing a parameter, all other experimental factors were kept constant.

2.2.1. Adsorption Isotherm and Kinetic Studies

Adsorption capacity (q_e, mg g^{-1}) and adsorbate concentration (C_e, mg L^{-1}) were linked during the adsorption equilibrium studies in liquid state. These adsorption isotherms indicate the critical dosage required for optimization of adsorbent concentration and how adsorbent interacts with adsorbate [20]. To understand the complex nature of adsorption system, various adsorption isotherms modeling was applied including Freundlich isotherm, Langmuir isotherm, Temkin isotherm, Dubinin Radushkevich isotherm, and Harkin–Jura isotherm.

Freundlich model gives information about heterogeneous, non-ideal and reversible adsorption. Linear form of Freundlich adsorption isotherm model is as follows:

$$lnq_e = \left(\frac{1}{n}\right) lnC + lnK_f \tag{3}$$

Langmuir adsorption model show single layer adsorption and the amount of adsorbent adsorbed is maximum for single layer. Linear form of Langmuir adsorption isotherm model is as follows:

$$\frac{C_e}{Q_e} = \frac{1}{Q^o K_t} + \frac{C_e}{Q^o} \tag{4}$$

To calculate Gaussian energy distributed on the heterogeneous surface during adsorption process Dubinin isotherm was used. Linear form of this model is as follows:

$$ln\ q_e = ln\ q_o - \beta\varepsilon^2 \tag{5}$$

where β (mol^2/J^2) is the activity coefficient and ε is the Polanyi potential and can be calculated from the following equation.

$$\varepsilon = RTLn(1 + \frac{1}{C_e}) \tag{6}$$

where R is the general gas constant and T is the absolute temperature in kelvin. Moreover, β value can be used to calculate mean free energy of adsorption from given equation:

$$E = 1/\sqrt{2\beta} \tag{7}$$

Another adsorption model called Temkin model was applied for non-distinguishable dispersal of binding energy on the surface of adsorbent. Linear form of this model is given as:

$$q_e = BlnA_t + BlnC_e \tag{8}$$

where A_t is the equilibrium constant and C_e is the concentration of adsorbent at equilibrium in mg/L.

Multilayer adsorption on the heterogenous porous surface of the adsorbent can be demonstrated by Harkin-Jura isotherm [17]. Its linear form is given as:

$$\frac{1}{q_e^2} = \frac{B}{A} - \left(\frac{1}{A}\right) logC_e \tag{9}$$

where A and B are the Harkin-Jura constants.

2.2.2. Adsorption Kinetics

Kinetic modeling for pseudo 1st- and pseudo 2nd-order reaction was performing after obtaining the experimental data through subsequent equations. Pseudo 1st-order reaction alternatively known as the Lagergren kinetic equation, which is extensively used to test the adsorption reactions' kinetic behavior.

$$\log(q_e - q_t) = \left[\log q_e - \left\{\frac{k_{\,1,ads}\, t}{2.303}\right\}\right] \tag{10}$$

where q_t and q_e are the dye's amounts adsorbed at equilibrium, and t is the time and $k_{1,ads}$ is the rate constant for pseudo 1st order reaction having units min^{-1}.

The pseudo 2nd-order reaction gives the information about rate limiting step that can be chemisorption and it involves the complete transfer or sharing of valance electron between adsorbate and adsorbent [21]. It is expressed as:

$$\frac{t}{q} = \frac{1}{k_{2,ads}q_e{}^2} + \frac{t}{q_t} \tag{11}$$

where, $k_{2,\,ads}$ are the pseudo 2nd order equilibrium rate constant having units g mol^{-1} min^{-1}.

3. Results and Discussion

3.1. Spectrophotometric Analysis

Spectrophotometric analysis was performed with UV-visible spectrophotometer to calculate the maximum absorption wavelengths for four dyes under study. The solution (100 ppm) of each dye was prepared, and absorbance was recorded from 335 nm to 1000 nm using appropriate blank solution. The maximum absorption wavelengths were as follows: 668 nm for Reactive Green-5 dye, 549 nm for Direct violet-51 dye, 515 nm for Reactive Red dye, and 507 nm for Acid Red dye (Figure 1).

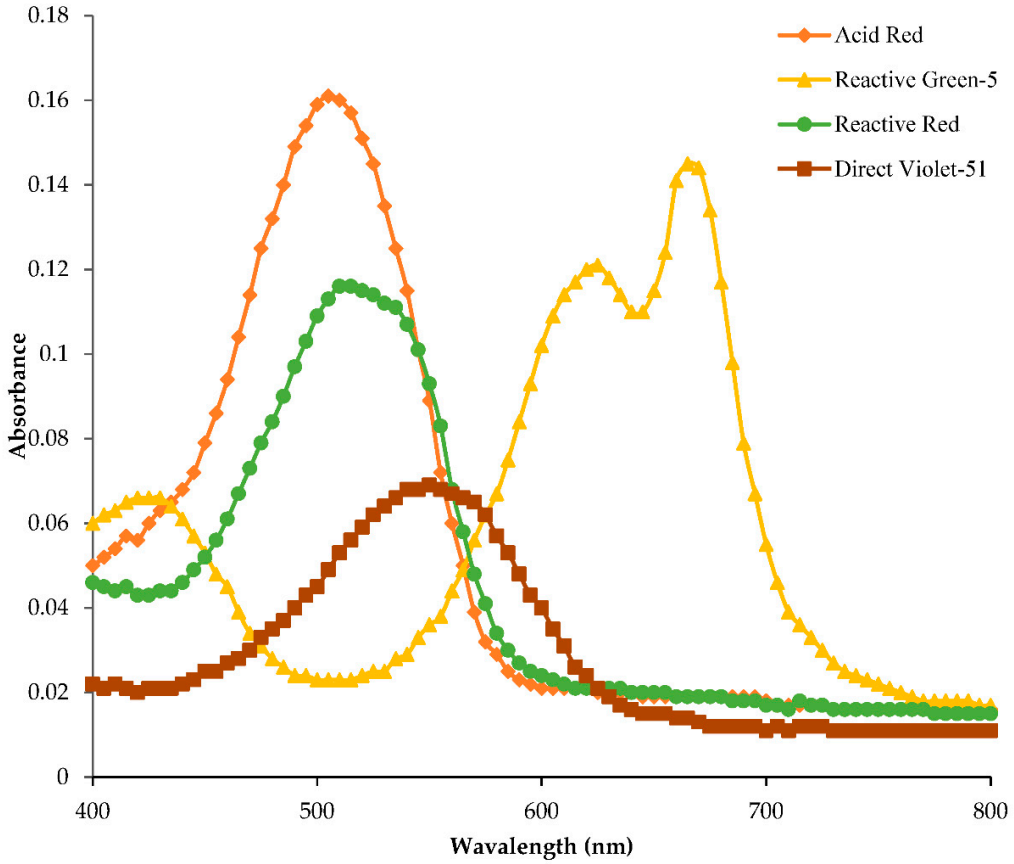

Figure 1. The determination of maximum absorption wavelengths for dyes.

3.2. Effect of Initial Dye Concentration

Initial dye concentration is responsible for the mass transfer between aqueous and solid phases because it provides the driving force. Increase in initial dye concentration may increase or decrease the percentage dye removal depending on the nature of dye (i.e., cationic or anionic). The amount of dye (mg/g) removed increases with increases in initial dye concentration [22]. Different concentration solutions (5, 10, 15, 25, and 50 ppm), of all four dyes (Reactive red, Direct violet-51, Reactive green-5, and Acid red dye) were prepared and analyzed after the shaking with different combinations of modified bentonite adsorbent (sodium metasilicate and potassium ferricyanide) (Figure 2). The results obtained

from spectrophotometer were utilized to make adsorption capacity graph for different adsorbents [23]. Bentonite treated with sodium metasilicate removed 68% of reactive red dye, bentonite treated with sodium metasilicate and potassium ferricyanide removed 62% of reactive red dye, and both pure bentonite and bentonite treated with potassium ferricyanide removed 60% of reactive red dye from the solution.

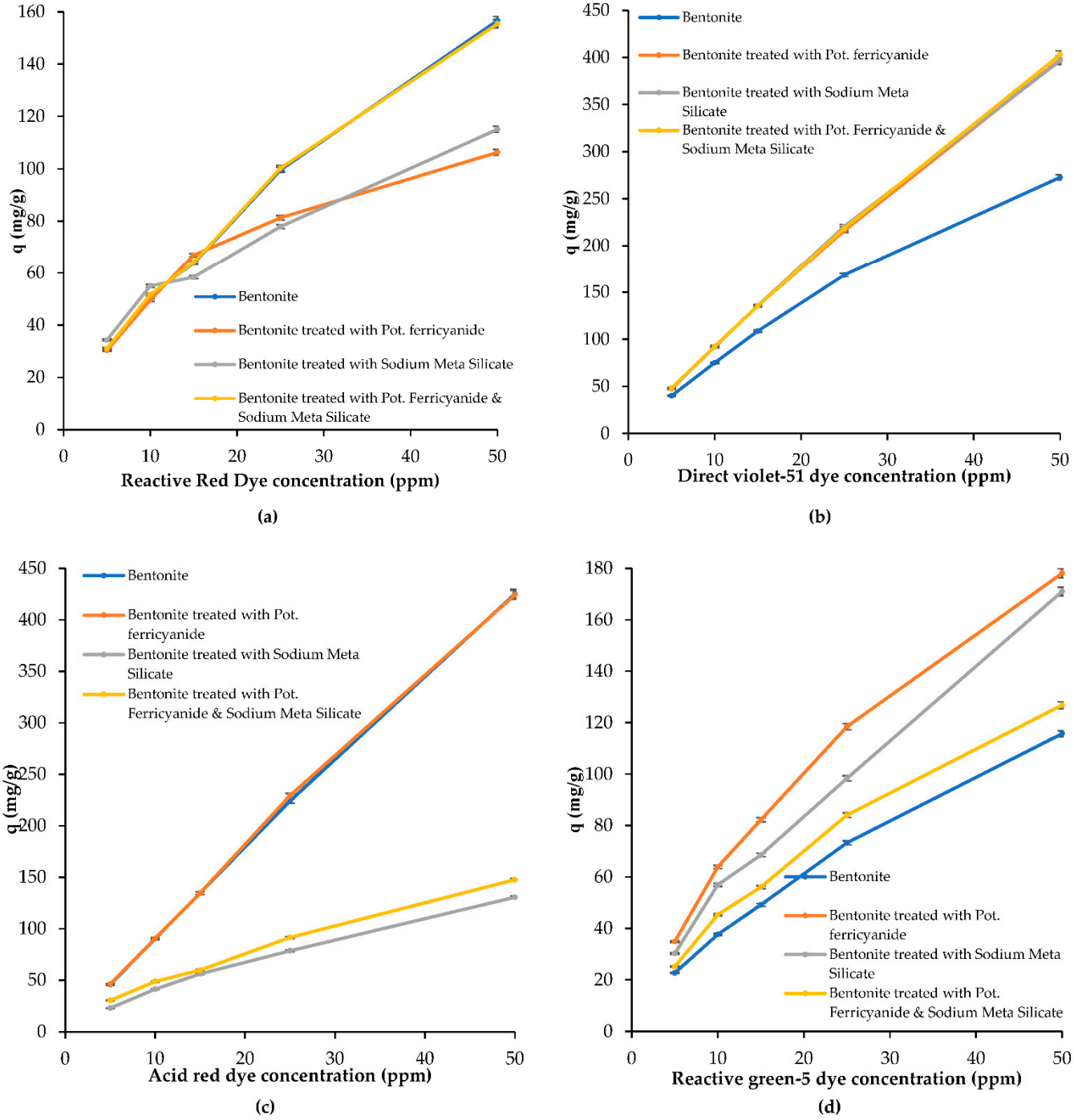

Figure 2. Adsorption capacities of adsorbents for (**a**) Reactive red, (**b**) Direct violet-51, (**c**) Acid red, and (**d**) Reactive green-5 dyes at different concentrations.

Bentonite treated with sodium metasilicate and potassium ferricyanide removed 96.6% of direct violet-51 dye, bentonite treated with sodium metasilicate removed 95%, bentonite treated with potassium ferricyanide removed 94%, and pure bentonite removed 80% of

the dye from the solution. Bentonite treated with potassium ferricyanide removed 92%, bentonite treated with sodium metasilicate removed 45.7%, bentonite treated with sodium metasilicate and potassium ferricyanide removed 60.6%, and pure bentonite removed 91% of acid red dye from the solution. Bentonite treated with potassium ferricyanide removed 69%, bentonite treated with sodium metasilicate removed 60%, bentonite treated with sodium metasilicate and potassium ferricyanide removed 50% and pure bentonite removed 45% of reactive green-5 dye solution.

3.3. Effect of Adsorbent Dosage

The determination of the effect of adsorbent dose is very important because it estimates the capacity of adsorbent to remove the amount of dye. Initially the amount of dye adsorption increases because of empty active sites on the adsorbent surface [20]. Once the equilibrium was attained, desorption started as it is clearly evident from the graphs in Figure 3. This was because of the overlapping of active sites of adsorbent with their own molecules. The removal of all four dyes from 50 ppm dye solution with four different adsorbents (bentonite treated with sodium metasilicate, bentonite treated with potassium ferricyanide, bentonite treated with sodium metasilicate and potassium ferricyanide, and pure bentonite) at varying doses 0.05, 0.1, 0.2, 0.3, and 0.4 g while keeping all other parameters constant was observed. Figure 3a shows the effect of dose on reactive red dye, while Figure 3b–d are showing the effect of dose on Direct violet-51, Acid red, and Reactive green-5 dyes at different adsorbent dosage.

3.4. Effect of Contact Time

The effect of contact time was observed at a variety of temperatures for each solution using 0.05 mg dose of adsorbents at 30, 40, 50, 60, and 70 °C at varying times: 15, 30, 60, 120, 240 min while keeping all other parameters constant. The amount of dye removed (mg/g) increased with increase in contact time. After gaining equilibrium at certain times, it became constant because all the active sites were occupied. Different temperatures were used to disturb the equilibrium and its re-establishment.

It is evident from Figure 4a that pure bentonite showed maximum efficiency at 70 °C in case of acid red dye, but bentonite treated with mixture of sodium metasilicate and potassium ferricyanide showed more efficient results in the presence of direct violet-51 dye, Figure 4b. Furthermore, bentonite treated with potassium ferricyanide and sodium metasilicate showed maximum absorption at 70 °C for reactive red dye solution, Figure 4c while bentonite treated with potassium ferricyanide and mixture of sodium metasilicate and potassium ferricyanide showed almost same absorption pattern, Figure 4d for reactive green-5 dye. All of them established equilibrium after 240 min.

3.5. Effect of Temperature

Temperature is one of the important variables in natural water system. Change in temperature affect the adsorption process in two ways; either before attaining the equilibrium or after attaining the equilibrium. Adsorption of dyes can be endothermic or exothermic process [24]. The effect of temperature at 30, 40, 50, 60, and 70 °C.

Figure 5a–d shows the adsorption of dyes using various adsorbents by fixing other parameters. Figure 5a shows the maximum adsorption of reactive red dye at 70 °C with modifier sodium metasilicate and potassium ferricyanide and Figure 5b,c shows adsorption capacities of acid red, and reactive green-5 at 60 and 70 °C, respectively. In case of direct violet-51 dye, bentonite treated with sodium metasilicate absorbed higher amount of dye from the solution at 40 and 50 °C as shown in Figure 5d. Above this temperature the composite active sites denatured hence the process of desorption starts. It indicates that direct violet-51 dye adsorption using composite materials was a highly exothermic reaction.

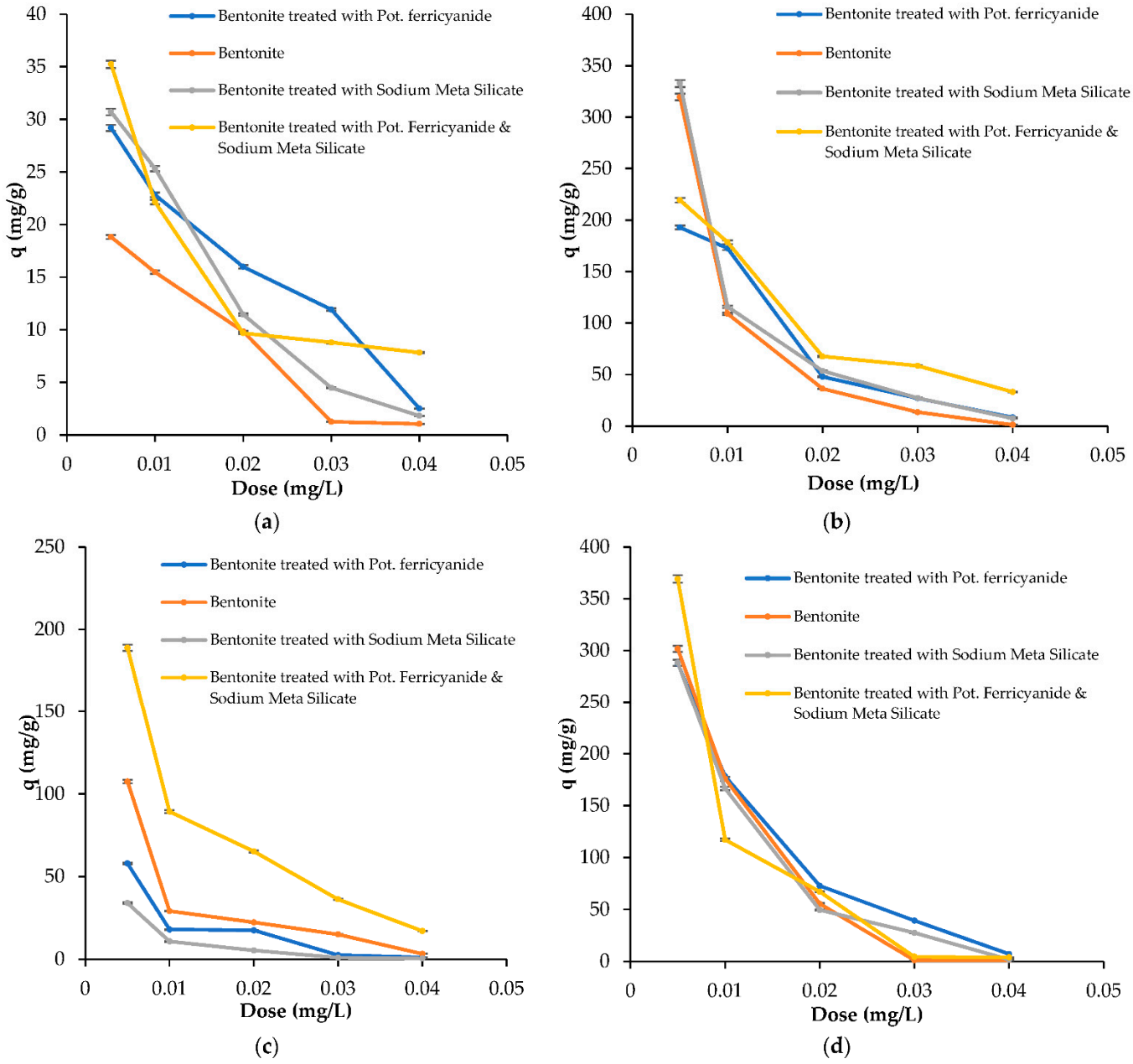

Figure 3. Adsorption capacities of adsorbents for (**a**) Reactive red, (**b**) Direct violet-51, (**c**) Acid red, and (**d**) Reactive green-5 dyes at different adsorbent dosage.

3.6. Effect of pH

The process of adsorption is also affected by the change in pH because it changes the chemical structure of both the adsorbent and the adsorbate. Anionic dye adsorption is generally favored by the negatively charged adsorbent's surfaces at low pH values or in acidic media. On the other hand, cationic dyes show more adsorption at high pH values. Bentonite as a whole is neutral but when was treated with sodium metasilicate, the surface become anionic due to which anionic dyes showed more adsorption at low pH values.

In case of acidic red and reactive red dye they show more adsorption with sodium metasilicate at lower pH values than other adsorbents as shown in graph as presented in Figure 6a,c. This is because of the anionic nature of the acid red and reactive red dye, while the rest of dyes i.e., reactive green-5 and direct violet-51 are cationic in nature, which is why they showed less adsorption at lower pH as indicated in Figure 6b,d.

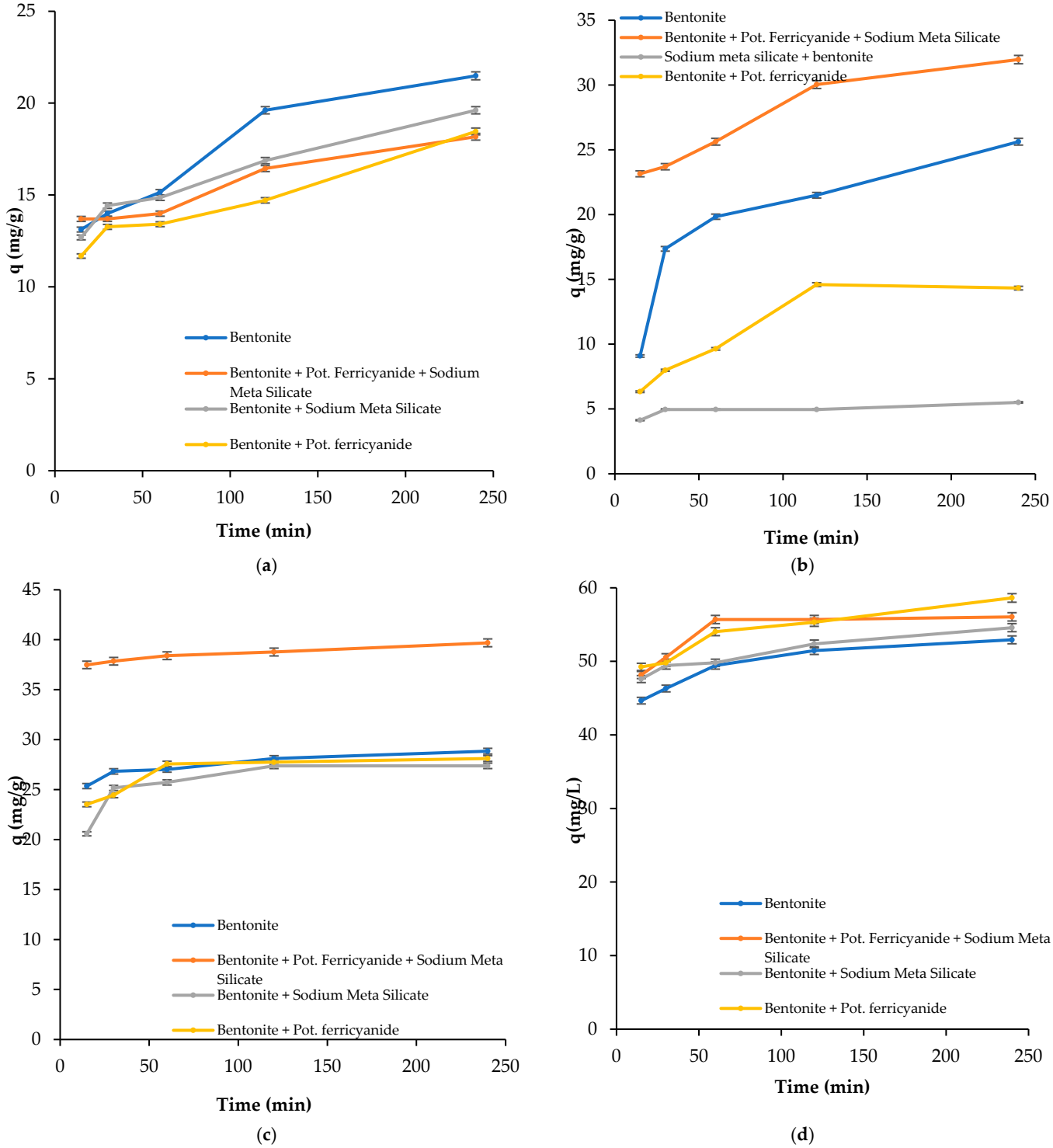

Figure 4. Adsorption capacities of adsorbents for (**a**) Acid red dye, (**b**) Direct violet-51, (**c**) Reactive red, and (**d**) Reactive green-5 dyes at varying contact times keeping the temperature 70 °C.

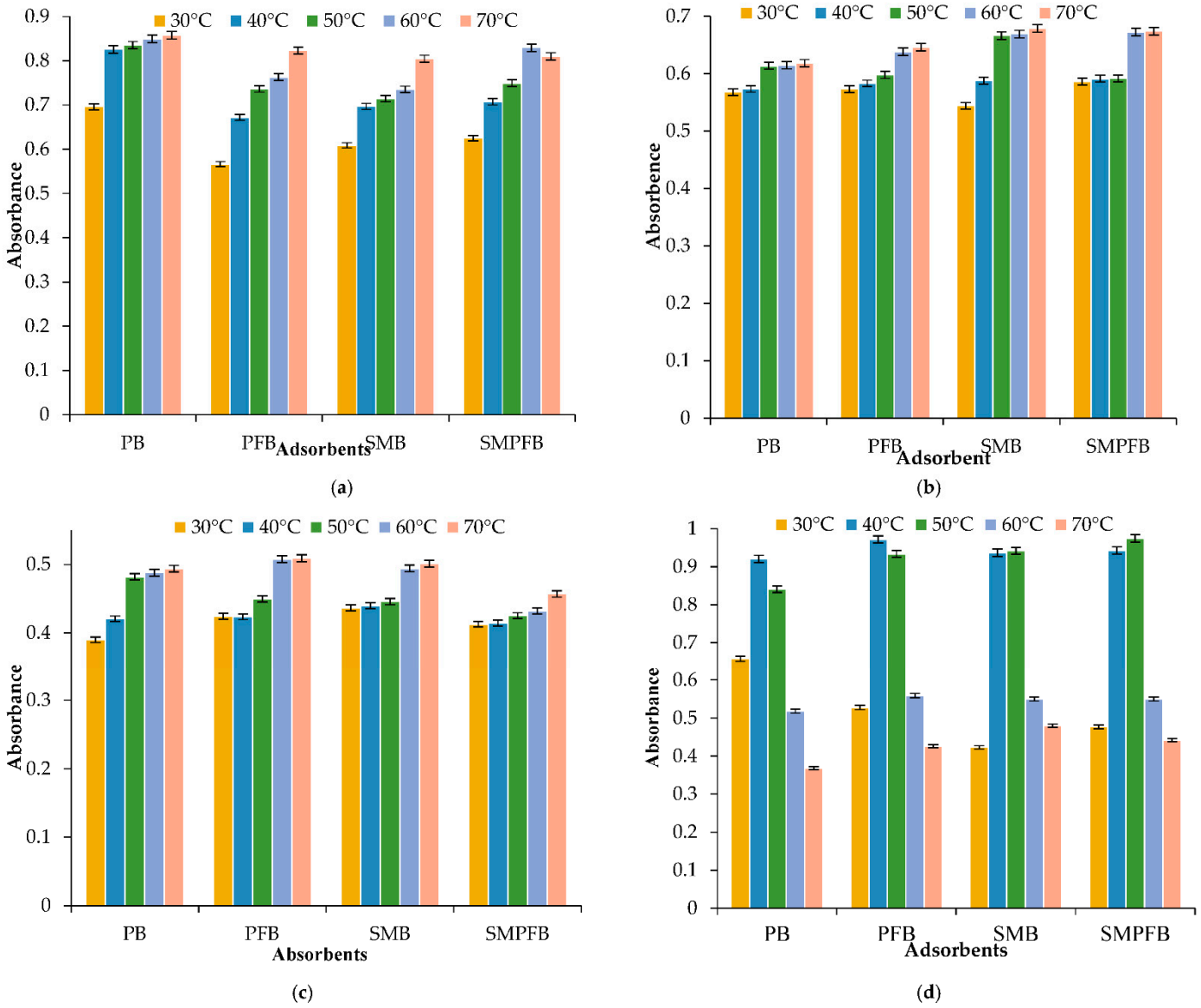

Figure 5. Removal of dyes at different temperatures. (**a**) Reactive Red, (**b**) Acid Red, (**c**) Reactive Green-5, (**d**) Direct Violet-51.

3.7. Isothermal Adsorption Models

To understand the mechanism of adsorption reactions, adsorption data or equilibrium data is very important. Five different isothermal models including Freundlich isotherm, Langmuir isotherm, Harkin-Jura, Temkin, and Dubinin Radushkevich isotherms were applied to the data (Table 1). The best fit model was Freundlich isotherm model for all the dyes under study. Freundlich isotherm model possessed the highest regression coefficient values i.e., $1 > R^2 > 0.96$. The difference between experimental and estimated *qe* (mg/g) values was also smaller for this model. These results signify that the adsorption process showed by the Acid red dye, Direct violet-51, Reactive red, and Reactive green-5 dye was a multilayered process [25].

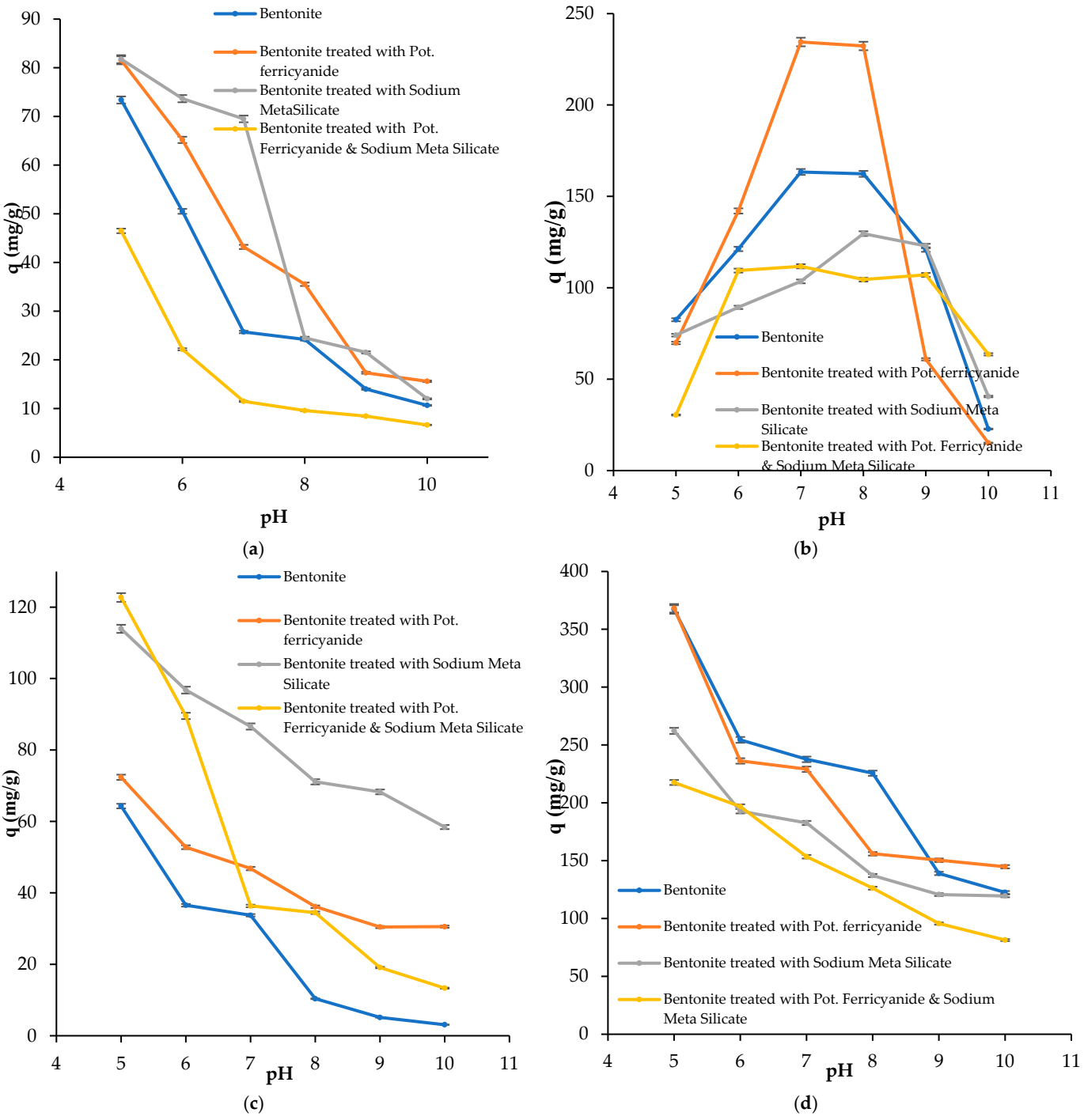

Figure 6. Adsorption capacities of adsorbents for (**a**) Acid red, (**b**) Direct violet-51, (**c**) Reactive red, and (**d**) Reactive green-5 dyes at varied pH.

Pure bentonite showed the highest regression coefficient when treated with reactive green-5 as evident from the Table 1. In the case of reactive red dye, the composite mixture having bentonite, sodium metasilicate, and potassium ferricyanide showed the highest regression coefficient, while direct violet-51 and acid red dye showed highest regression coefficient for bentonite treated with potassium ferricyanide and bentonite treated with sodium metasilicate as indicated in Table 1.

Table 1. Experimental data of adsorption isotherms for all dyes.

Adsorption Isotherms																		
Dyes	**Langmuir Isotherm**					**Freundlich Isotherm**				**Dubinin Radushkevich Isotherm**				**Temkin Isotherm**			**Harkin–Jura Isotherm**		
Reactive Green-5 Dye	Adsorbents	Q_{exp} (mg/g)	R^2	Q_{cal}	K_L	R^2	Q_{cal}	K_f	n	R^2	Q_{cal}	β	E	R^2	A_t	B	R^2	A	B
	Bentonite	115.7	0.950	181.8	0.042	0.999	112.5	12.1	1.6	0.710	72.3	2×10^{-6}	500	0.937	0.53	35.04	0.820	625	1.4
	BPF	178.1	0.979	227.3	0.098	0.992	185.2	30.1	1.9	0.771	116.6	8×10^{-7}	1000	0.729	0.03	74.64	0.677	19.1	1.7
	BSM	171.0	0.895	243.9	0.058	0.983	164.3	21.3	1.7	0.742	104	1×10^{-6}	707	0.567	0.04	37.42	0.865	10.5	1.7
	BSMPF	126.9	0.971	185.2	0.055	0.992	131.0	15.4	1.6	0.764	83.29	2×10^{-6}	500	0.96	0.64	37.26	0.769	833.3	1.4
Reactive Red Dye	Bentonite	156.7	0.928	227.3	0.006	0.99	154.5	20.5	1.8	0.685	95.21	1×10^{-6}	707	0.92	0.76	43.47	0.326	6.87	1.6
	BPF	106.3	0.995	123.5	0.011	0.973	114	24.7	2.4	0.813	80.17	1×10^{-6}	707	0.994	1.63	25.42	0.766	0.72	1.7
	BSM	115.1	0.947	131.6	0.426	0.969	108.9	29.3	1.7	0.675	77.8	6×10^{-7}	913	0.906	2.1	23.62	0.871	2000	1.6
	BSMPF	155.4	0.929	222.2	0.093	0.992	152.9	21.2	1.8	0.674	94.6	1×10^{-6}	707	0.919	0.79	42.56	0.864	25.38	-1
Acid Red Dye	Bentonite	425.2	0.978	909.1	0.118	0.992	460.3	93.4	1.3	0.807	252.3	2×10^{-7}	1581	0.935	0.06	19.4	0.689	2500	0.5
	BPF	424.3	0.888	833.3	0.14	0.968	472.7	100	1.3	0.781	253.9	2×10^{-7}	1581	0.489	0.21	3.73	0.335	9.9	1.8
	BSM	130.6	0.962	212.8	0.040	0.997	131.8	12.4	1.5	0.762	82.1	2×10^{-6}	500	0.182	0.22	7.47	0.761	666.7	1.4
	BSMPF	147.6	0.899	212.8	0.057	0.988	140	19.9	1.8	0.639	87.5	1×10^{-6}	707	0.118	0.85	135.6	0.027	666.7	52
Direct Violet-51 Dye	Bentonite	272.8	0.991	384.6	0.10	0.991	29.37	42.6	1.6	0.757	165.2	5×10^{-7}	1000	0.961	1.28	75.6	0.722	2500	13
	BPF	397.8	0.961	526.3	0.29	0.998	11.75	106	1.7	0.771	227.3	1×10^{-7}	2236	0.924	4.8	94.8	0.704	204.1	1.9
	BSM	396.7	0.969	526.3	0.27	0.996	11.09	110	1.7	0.727	218.7	9×10^{-8}	2357	0.919	4.58	92.4	0.748	5000	1
	BSMPF	402.9	0.927	526.3	0.302	0.995	38.59	116	1.9	0.688	210.7	7×10^{-8}	2673	0.871	5.72	85.8	0.803	5000	1

3.8. Kinetic Adsorption Models

3.8.1. Pseudo 1st-Order Model

The values of q_e and k_1 were calculate (ed from intercept and slop of the plotted graph between time (t) and log ($q_e - q_t$). The difference obtained between the experimental and calculated q and R^2 showed that these dyes were not following pseudo 1st-order kinetics (Table 2).

Table 2. (**a**) Adsorption kinetics data for Reactive green-5 dye. (**b**) Adsorption kinetics data for Reactive red dye. (**c**) Adsorption kinetics data for Acid red dye. (**d**) Adsorption kinetics data for Violet-51 dye.

(**a**)

Reactive Green-5 Dye	**Adsorption Kinetics**							
Adsorbents	**Pseudo 1st Order Kinetics**				**Pseudo 2nd Order Kinetics**			
	30 °C							
	Q_{exp}	$Q°$	K_1	R^2	Q_{exp}	$Q°$	K_2	R^2
Bentonite	275.7	70.37	0.016	0.864	275.7	277.8	0.0005	0.997
BPF	257.1	43.36	0.019	0.754	257.1	263.2	0.0008	0.999
BSM	261.5	32.20	0.015	0.926	261.5	263.2	0.0013	1
BSMPF	311.2	103	0.018	0.952	311.2	322.6	0.0004	0.999
	40 °C							
Bentonite	292.1	148.15	0.016	0.958	292.1	294.12	0.0008	0.999
BPF	352.1	52.77	0.019	0.869	352.1	357.14	0.0003	0.994
BSM	223.2	120.1	0.018	0.933	223.2	232.56	0.0003	0.996
BSMPF	373.2	90.80	0.017	0.889	373.2	370.4	0.0005	0.998
	50 °C							
Bentonite	759.1	95.74	0.018	0.940	759.1	769.2	0.0005	0.999
BPF	832.2	217.5	0.022	0.986	832.2	833.3	0.0002	0.999
BSM	744.3	19.94	0.012	0.932	744.3	769.2	0.0007	0.999
BSMPF	760.1	96.72	0.018	0.947	760.1	769.2	0.0005	0.999
	60 °C							
Bentonite	738	91.47	0.018	0.949	738	769.2	0.0005	0.999
BPF	746.1	42.28	0.015	0.987	746.1	769.2	0.0010	1
BSM	728.9	66.62	0.017	0.969	728.9	714.3	0.0007	0.999
BSMPF	746.1	41.23	0.017	0.899	746.1	769.2	0.0009	1
	70 °C							
Bentonite	669.8	23.56	0.015	0.811	669.8	666.7	0.0017	1
BPF	685.4	27.4	0.015	0.96	685.4	714.3	0.0015	1
BSM	671.9	69.15	0.016	0.907	671.9	666.7	0.0006	0.999
BSMPF	690.5	23.63	0.015	0.852	690.5	666.7	0.0019	1

(**b**)

Reactive Red Dye	**Adsorption Kinetics**							
Adsorbents	**Pseudo 1st Order Kinetics**				**Pseudo 2nd Order Kinetics**			
	30 °C							
	Q_{exp}	$Q°$	K_1	R^2	Q_{exp}	$Q°$	K_2	R^2
Bentonite	204.5	62.82	0.0184	0.912	204.5	212.77	0.0004	0.998
BPF	117.8	92.0	0.017	0.863	117.8	123.46	0.0003	0.960
BSM	154.5	52.52	0.0147	0.853	154.5	156.25	0.0007	0.993
BSMPF	199.4	21.20	0.0147	0.644	199.4	204.1	0.0010	0.999

Table 2. *Cont.*

				40 °C				
Bentonite	138.6	34.94	0.013	0.886	138.6	140.8	0.0010	0.996
BPF	142.5	19.84	0.015	0.796	142.5	144.9	0.0017	0.999
BSM	173.2	25.59	0.017	0.654	173.2	175.4	0.0013	0.999
BSMPF	155.4	54.45	0.015	0.909	155.4	158.7	0.0007	0.996
				50 °C				
Bentonite	169.2	26.79	0.014	0.999	169.2	172.4	0.0014	0.999
BPF	149.6	33.88	0.015	0.977	149.6	151.5	0.0011	0.999
BSM	147.3	34.59	0.014	0.93	147.3	149.3	0.0011	0.999
BSMPF	164	25.72	0.014	0.977	164	166.7	0.0015	0.999
				60 °C				
Bentonite	375.9	36.74	0.0140	0.924	375.9	384.6	0.0011	0.999
BPF	309	19.48	0.0131	0.903	309	312.5	0.002	1
BSM	390.5	120.22	0.0187	0.944	390.5	416.7	0.0004	0.999
BSMPF	406.5	57.58	0.0175	0.987	406.5	400	0.0008	1
				70 °C				
Bentonite	141.1	16.89	0.011	0.933	141.1	142.86	0.0021	0.999
BPF	163.3	88.69	0.0177	0.965	163.3	169.49	0.0004	0.997
BSM	185	122.7	0.0193	0.987	185	196.08	0.0003	0.999
BSMPF	234.98	117.5	0.0189	0.968	234.98	243.9	0.0003	0.998

(**c**)

Acid Red Dye	**Adsorption Kinetics**							
Adsorbents	**Pseudo 1st Order Kinetics**				**Pseudo 2nd Order Kinetics**			
	30 °C							
	Q_e	$Q°$	K_1	R^2	Q_e	$Q°$	K_2	R^2
Bentonite	149.1	46.68	0.016	0.997	149.1	153.9	0.0008	0.999
BPF	133.1	31.25	0.014	0.973	133.1	135.1	0.0011	0.999
BSM	146.4	34.98	0.014	0.929	146.4	149.3	0.0010	0.998
BSMPF	154.8	70	0.016	0.912	154.8	158.7	0.0005	0.994
				40 °C				
Bentonite	317.7	162.9	0.023	0.932	317.7	344.8	0.0002	0.997
BPF	270.3	153.2	0.020	0.954	270.3	285.7	0.0003	0.996
BSM	250.3	31	0.015	0.921	250.3	256.4	0.0013	1
BSMPF	180	41	0.019	0.751	180	185.2	0.0008	0.999
				50 °C				
Bentonite	198.2	73.81	0.018	0.982	198.2	204.1	0.0005	0.999
BPF	243.6	84.76	0.017	0.938	243.6	250	0.0004	0.998
BSM	181.3	65.4	0.018	0.988	181.3	188.7	0.0006	0.999
BSMPF	137.9	12.7	0.010	0.970	137.9	138.9	0.0027	0.999
				60 °C				
Bentonite	274.4	38.1	0.014	0.934	274.4	277.8	0.0010	0.999
BPF	363.6	102.4	0.019	0.952	363.6	370.3	0.0004	0.999
BSM	323.1	74.5	0.016	0.867	323.1	322.6	0.0005	0.998
BSMPF	284.1	50.4	0.017	0.956	284.1	285.7	0.0008	0.999
				70 °C				
Bentonite	189.6	56.9	0.020	0.773	189.6	196.1	0.0006	0.997
BPF	163.7	80.7	0.017	0.890	163.7	169.5	0.0004	0.991
BSM	181.6	64.4	0.017	0.971	181.6	185.2	0.0006	0.999
BSMPF	162.8	52.6	0.015	0.939	162.8	166.7	0.0007	0.997

Table 2. *Cont.*

(**d**)								
Direct Violet-51 Dye	**Adsorption Kinetics**							
Adsorbents	**Pseudo 1st Order Kinetics**				**Pseudo 2nd Order Kinetics**			
	30 °C							
	Q_e	$Q°$	K_1	R^2	Q_e	$Q°$	K_2	R^2
Bentonite	186.5	89.0	0.017	0.895	186.5	192.3	0.0004	0.993
BPF	162.7	85.3	0.018	0.990	162.7	147.0	0.0004	0.996
BSM	172.6	74.4	0.017	0.952	172.6	178.5	0.0005	0.998
BSMPF	136.8	150.1	0.020	0.965	136.8	181.8	0.0002	0.998
	40 °C							
Bentonite	104.9	64.66	0.019	0.871	104.9	129.9	0.0002	0.987
BPF	132.2	24.8	0.015	0.842	132.2	135.1	0.0012	0.999
BSM	153.6	17.52	0.015	0.601	153.6	158.7	0.0012	0.999
BSMPF	107.3	132.1	0.020	0.980	107.3	138.9	0.0001	0.979
	50 °C							
Bentonite	178.7	21.98	0.0138	0.907	178.7	188.7	0.0044	0.998
BPF	141.4	99.40	0.0177	0.941	141.4	149.2	0.0003	0.992
BSM	100.5	32.12	0.0172	0.720	100.5	105.2	0.0008	0.998
BSMPF	172.3	25.06	0.0161	0.693	172.3	178.5	0.0006	0.999
	60 °C							
Bentonite	163.9	122.8	0.020	0.994	163.9	187.8	0.0002	0.998
BPF	180.9	86.47	0.017	0.933	180.9	188.7	0.0004	0.996
BSM	213.2	191.9	0.020	0.908	213.2	243.9	0.0001	0.969
BSMPF	174.7	83.98	0.018	0.930	174.7	185.1	0.0004	0.997
	70 °C							
Bentonite	203	36.38	0.019	0.639	203	212.8	0.0005	0.996
BPF	141.1	133.2	0.020	0.989	141.1	161.3	0.0002	0.991
BSM	60.5	9.79	0.012	0.684	60.5	62.11	0.0030	0.999
BSMPF	239.2	25.79	0.012	0.893	239.2	238.1	0.0015	0.999

3.8.2. Pseudo 2nd Order Model

The values of q_e and k_1 were calculated from intercept and slop of the plotted graph between time (t) and t/q_t. Pseudo 2nd-order kinetics follow the assumption that the rate limiting step could be chemisorption which indicate the involvement of valance electron among the adsorbate and adsorbent through sharing or exchange of electrons. Adsorption capacities (q_e) calculated from the data were maximum during this case. Moreover, R^2 were also between 1 and 0.99 i.e., ($1 \geq R^2 > 0.99$). This indicated that all the dyes were obeying the pseudo 2nd order kinetics (Table 2).

Table 2a showed the values of adsorption kinetics for reactive green-5 dye and at maximum temperature of 70 °C showed the highest adsorption capacities for bentonites treated with sodium metasilicate and potassium ferricyanide (BSMPF) composite and bentonite treated with potassium ferricyanide (BPF) composite. Table 2b shows the results for reactive red dye for all the modified composites. Table 2c,d showed the adsorption capacities for acid red and direct violet-51 dyes and highest adsorption capacities for BSM and BSMPF, respectively [26].

3.9. Characterization of Bentonite

3.9.1. Scanning Electron Microscopy (SEM) Analysis

SEM has been used to see structure and surface topology of pure and modified bentonite nanocomposites. It explained much about the morphological modifications

that potassium ferricyanides and sodium metasilicate brought. Raw or pure bentonite had closely packed flakes due to which it appeared smooth in SEM image at 200 nm in Figure 7a [27].

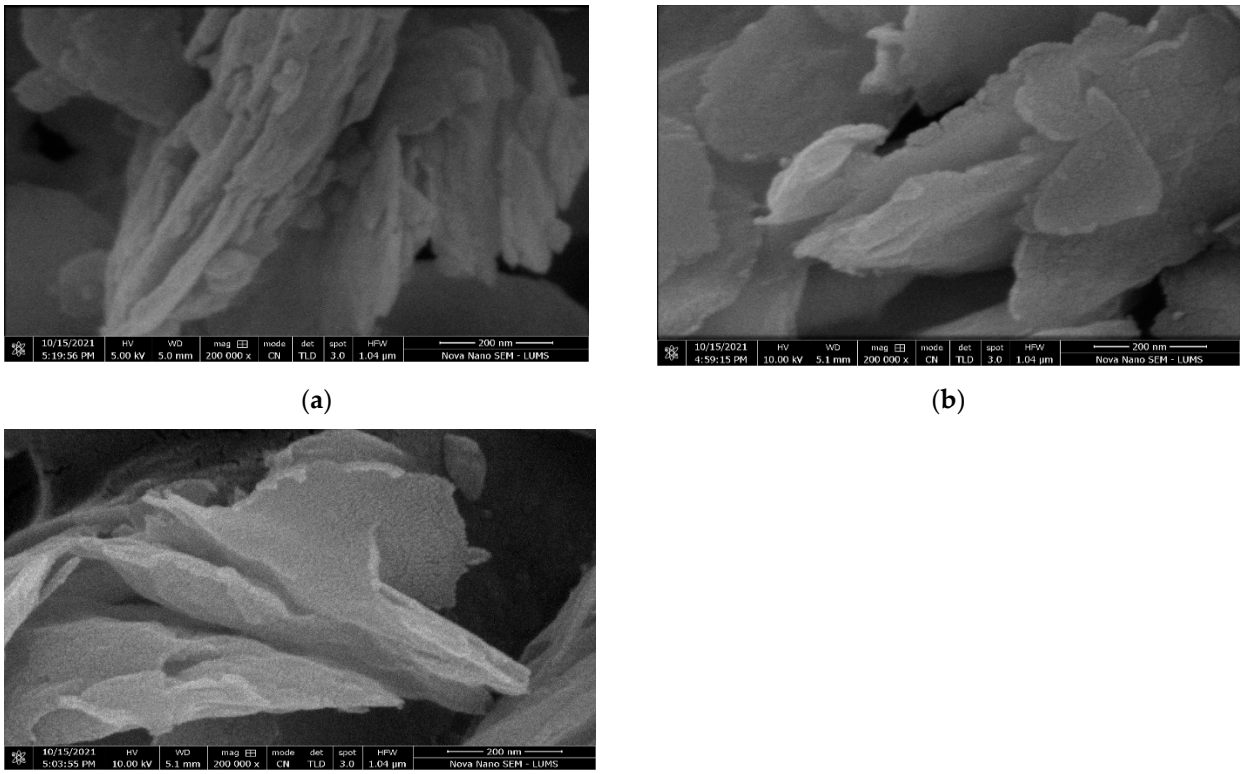

Figure 7. SEM images at 200 nm (**a**) pure bentonite (**b**) bentonite treated with sodium metasilicate (**c**) bentonite treated with sodium metasilicate and potassium ferricyanide.

While bentonite treated with sodium metasilicate, and bentonite treated with potassium ferricyanide and sodium metasilicate mixture had loosely bounded structure and allowing more binding sites for adsorption in Figure 7b,c, respectively. Bentonite treated with sodium metasilicate composite contained spherical particles and mixture composite of bentonite treated with potassium ferricyanide and sodium metasilicate showed spike like particles with heterogenous surface [28].

3.9.2. Fourier Transform Infrared (FTIR) Analysis

The Fourier transforms infrared spectrum of pure bentonite nanocomposite is presented in Figure 8. The adsorption spectrum of pure bentonite showed by the upper line indicated the adsorption at 3621 cm^{-1}, which indicate presence of OH group. This region is typical for montmorillonite to OH stretching vibrations that have Al and Mg coordination groups with octahedral layer. This characteristic band show interlayer hydrogen bonding in clay. Adsorption spectrum at 1436 cm^{-1}, and 978 cm^{-1} represent the CO_2 and Al-OH stretching respectively. The spectral band obtained at 796 cm^{-1} indicated the presence of low crystalline silica (SiO_4^{2-} tetrahedra) and cristobalite.

The FTIR spectrum of modified bentonite containing bentonite treated with sodium metasilicate (BSM) is presented in the Figure 8 lower spectral line. Adsorption bands were obtained at 3619, 1436, 974, 795, and 777 cm^{-1}, which indicated the stretching vibrations of OH groups, CO_2, Al-OH stretching, amorphous silica, and C-H deformation [29]. Figure 8 middle spectrum line shows the adsorption spectrum for bentonite treated with

sodium metasilicate and potassium ferricyanide at 3619, 1457, 974, 795, and 777 cm^{-1}, this combination shifts the methylene C-H bond bending [30].

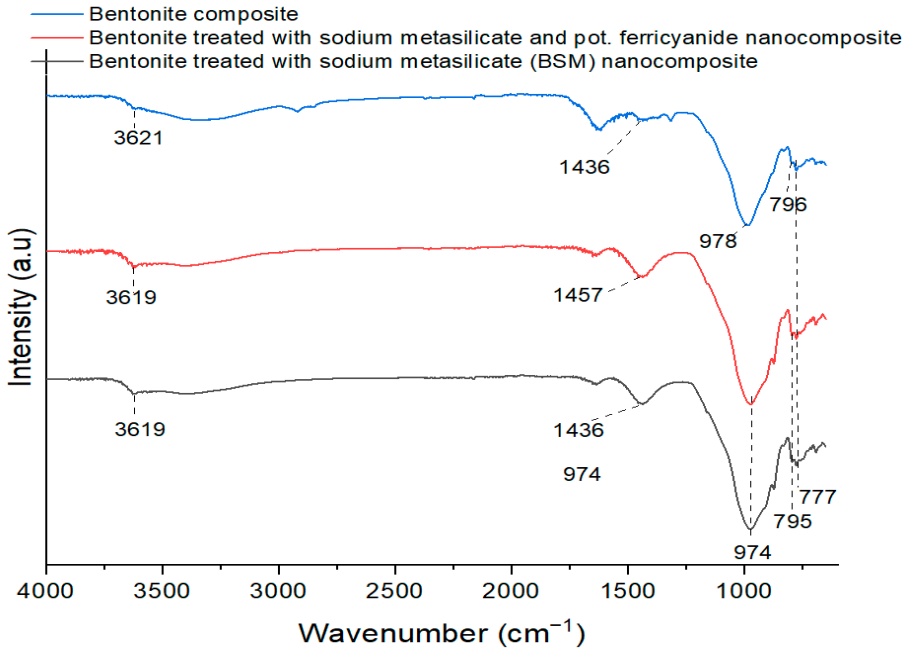

Figure 8. FTIR analysis of bentonite nanocomposite Bentonite treated with sodium metasilicate (BSM) nanocomposite bentonite treated with sodium metasilicate and potassim ferricyanide nanocomposite.

3.9.3. X-ray Diffraction (XRD) Analysis

Constructive interference was produced by the interaction of incident rays with the sample, and these diffracted rays are continually recorded by the detectors. Cu-kα radiations were used over 2θ rages from 20 to 60 degrees at a speed of 2 deg min^{-1} for the characterization of modified bentonite. This XRD analysis of pure bentonite showed the monmorrilonit, kaolinite, and cristobalite composition as presented in Figure 9.

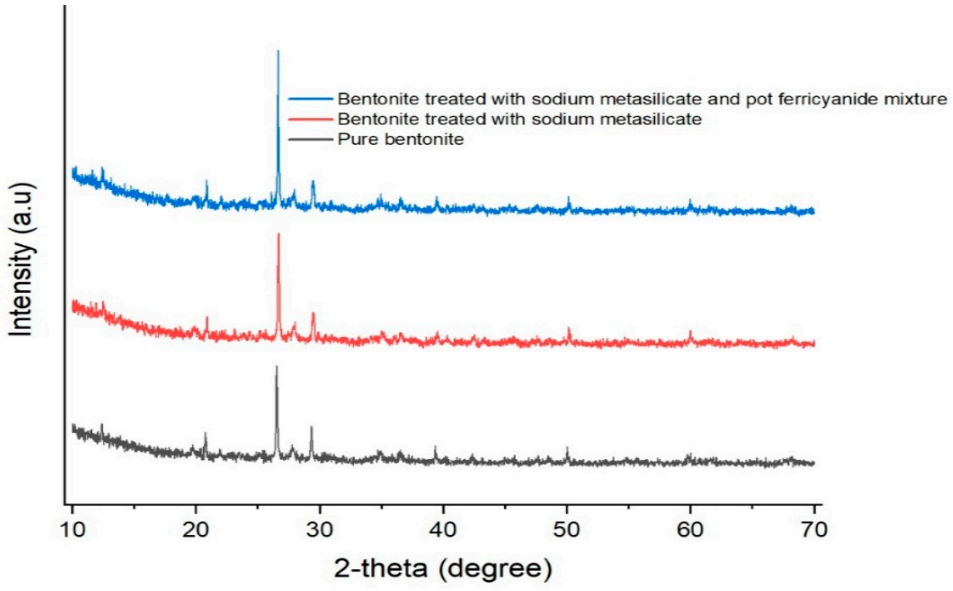

Figure 9. XRD analysis of bentonite nanocomposite, bentonite treated with sodium meta-silicate (BSM) nanocomposite, bentonite treated with sodium metasilicate and pot. ferricyanide nanocomposite.

3.9.4. Desorption

It is a physical process in which a previously adsorbed substance is removed from the surface of the adsorbent. Desorption studies were conducted for adsorbents used in the present study. No significant loss in the adsorption capacity was observed after three cycles as presented in Figure 10.

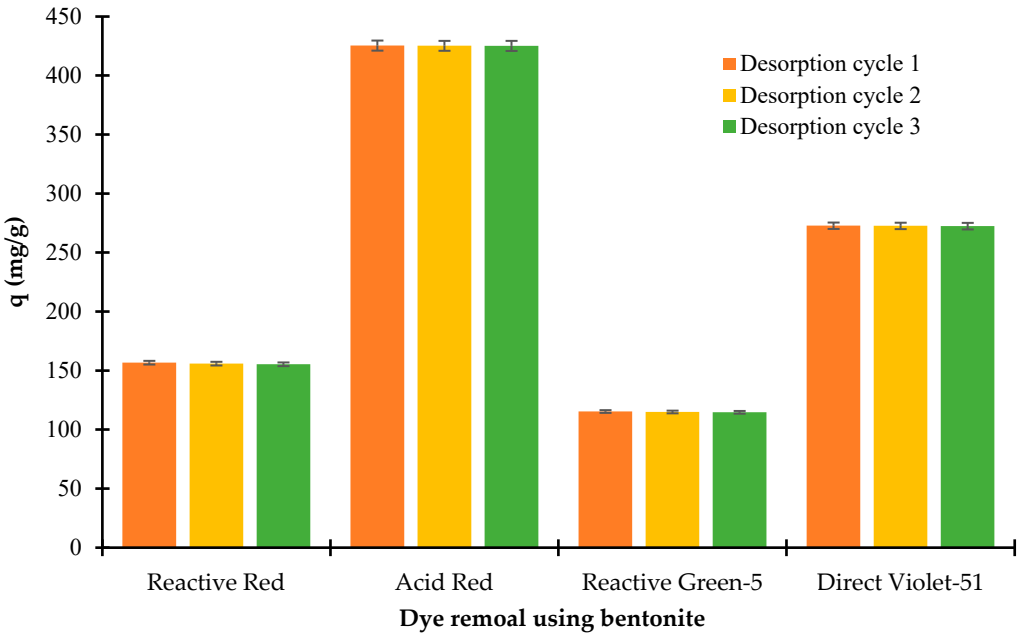

Figure 10. Adsorption capacity (mg/g) of adsorbent after desorption cycle.

4. Conclusions

Our environment is severely affected by contaminated wastewater released from textile industries. Bentonite clay is nature friendly, abundant, and cost-effective and its modification showed improvements in adsorption results. Removal efficiency was tremendously increased by increasing initial dye concentration, lowering the amount of adsorbent, lowering pH, varying time, and temperature. Moreover, the modification of bentonite with potassium ferricyanide and sodium metasilicate was a cheap process and could be used easily to replace expensive adsorbents like zeolite and activated carbon. It was found that Freundlich isotherm shown best fit model to the adsorption data, which signify that dye adsorption was multilayered. The best correlation for the obtained experimental data was shown by the pseudo second order kinetic model.

Author Contributions: Conceptualization, U.R. and M.A.H.; methodology, Y.C.; I.A.B.; U.R. and M.A.H.; software, U.R. and F.A.A.; validation, U.R., M.A.H., F.A.A., E.A.K. and Y.J.; formal analysis, Y.C., U.R., M.A.H., Y.J. and I.A.B.; investigation, U.R., M.A.H., Y.C., H.A. and F.A.A.; resources, U.R. and F.A.A.; data curation, U.R., Y.C., Y.J. and M.A.H.; writing—original draft preparation, Y.C., H.A. and M.A.H.; writing—review and editing, U.R., Y.J., F.A.A., I.A.B., E.A.K. and M.A.H.; visualization, M.A.H. and U.R.; supervision, M.A.H.; project administration, U.R., M.A.H. and F.A.A.; funding acquisition, U.R. and F.A.A. All authors have read and agreed to the published version of the manuscript.

Funding: The authors extend their thanks to Researchers Supporting Project (RSP-2021/160), King Saud University, Riyadh, Saudi Arabia.

Data Availability Statement: Not applicable.

Conflicts of Interest: The authors declare no conflict of interest.

References

1. Khan, S.; Malik, A. Environmental and health effects of textile industry wastewater. In *Environmental Deterioration and Human Health*; Springer: Berlin/Heidelberg, Germany, 2014; pp. 55–71.
2. Sivaram, N.; Gopal, P.; Barik, D. Toxic waste from textile industries. In *Energy from Toxic Organic Waste for Heat and Power Generation*; Elsevier: Amsterdam, The Netherlands, 2019; pp. 43–54.
3. Azizullah, A.; Khattak, M.N.K.; Richter, P.; Häder, D.-P. Water pollution in Pakistan and its impact on public health—A review. *Environ. Int.* **2011**, *37*, 479–497. [CrossRef] [PubMed]
4. Halder, J.N.; Islam, M.N. Water pollution and its impact on the human health. *J. Environ. Hum.* **2015**, *2*, 36–46. [CrossRef]
5. Shi, B.; Li, G.; Wang, D.; Feng, C.; Tang, H. Removal of direct dyes by coagulation: The performance of preformed polymeric aluminum species. *J. Hazard. Mater.* **2007**, *143*, 567–574. [CrossRef] [PubMed]
6. Kumar, P.S.; Saravanan, A. Sustainable wastewater treatments in textile sector. In *Sustainable Fibres and Textiles*; Elsevier: Amsterdam, The Netherlands, 2017; pp. 323–346.
7. Beulah, S.S.; Muthukumaran, K. Methodologies of removal of dyes from wastewater: A review. *Int. Res. J. Pure Appl. Chem.* **2020**, *50*, 68–78. [CrossRef]
8. Gupta, V.; Ali, I.; Saini, V.; Gerven, T.V.; der Bruggen, B.V.; Vandecasteele, C. Removal of dyes from wastewater using bottom ash. *Ind. Eng. Chem. Res.* **2005**, *44*, 3655–3664. [CrossRef]
9. Crini, G.; Lichtfouse, E.; Wilson, L.D.; Morin-Crini, N. Conventional and non-conventional adsorbents for wastewater treatment. *Environ. Chem. Lett.* **2019**, *17*, 195–213. [CrossRef]
10. Mukhopadhyay, R.; Bhaduri, D.; Sarkar, B.; Rusmin, R.; Hou, D.; Khanam, R.; Sarkar, S.; Biswas, J.K.; Vithanage, M.; Bhatnagar, A. Clay–polymer nanocomposites: Progress and challenges for use in sustainable water treatment. *J. Hazard. Mater.* **2020**, *383*, 121125. [CrossRef]
11. Apriandanu, D.O.B.; Yulizar, Y. CuO-bentonite-gold nanocomposites: Facile green preparation and their characterization. *Mater. Lett.* **2021**, *284*, 128911. [CrossRef]
12. Hu, Q.H.; Qiao, S.Z.; Haghseresht, F.; Wilson, M.A.; Lu, G.Q. Adsorption study for removal of basic red dye using bentonite. *Ind. Eng. Chem. Res.* **2006**, *45*, 733–738. [CrossRef]
13. Khelifi, S.; Ayari, F. Modified bentonite for anionic dye removal from aqueous solutions. Adsorbent regeneration by the photo-Fenton process. *Comptes. Rendus. Chim.* **2019**, *22*, 154–160. [CrossRef]
14. Tahir, S.S.; Rauf, N. Removal of a cationic dye from aqueous solutions by adsorption onto bentonite clay. *Chemosphere* **2006**, *63*, 1842–1848. [CrossRef] [PubMed]
15. Peng, Y.; Lu, R. An LCTF-based multispectral imaging system for estimation of apple fruit firmness: Part II. Selection of optimal wavelengths and development of prediction models. *Trans. ASABE* **2006**, *49*, 269–275. [CrossRef]
16. Gong, Z.; Liao, L.; Lv, G.; Wang, X. A simple method for physical purification of bentonite. *Appl. Clay Sci.* **2016**, *119*, 294–300. [CrossRef]
17. Mokhtar, A.; Abdelkrim, S.; Sardi, A.; Benyoub, A.; Besnaci, H.; Cherrak, R.; Hadjel, M.; Boukoussa, B. Preparation and characterization of anionic composite hydrogel for dyes adsorption and filtration: Non-linear isotherm and kinetics modeling. *J. Polym. Environ.* **2020**, *28*, 1710–1723. [CrossRef]
18. Davies, A.; Vadodaria, B.; Hopwood, B.; Dexter, T.; Conn, D. Efficacy of microfiltration in decreasing propofol-induced pain. *Anaesthesia* **2002**, *57*, 557–561. [CrossRef]
19. Khalil, M.; Hanif, M.A.; Rashid, U.; Ahmad, J.; Alsalme, A.; Tsubota, T. Low-cost novel nano-constructed granite composites for removal of hazardous Terasil dye from wastewater. *Environ. Sci. Pollut. Res.* **2022**. [CrossRef] [PubMed]
20. Ehrampoush, M.; Ghanizadeh, G.; Ghaneian, M. Equilibrium and kinetics study of reactive red 123 dye removal from aqueous solution by adsorption on eggshell. *J. Environ. Health Sci. Eng.* **2011**, *8*, 101–106.
21. Dada, A.; Olalekan, A.; Olatunya, A.; Dada, O. Langmuir, Freundlich, Temkin and Dubinin–Radushkevich isotherms studies of equilibrium sorption of Zn^{2+} unto phosphoric acid modified rice husk. *IOSR J. Appl. Chem.* **2012**, *3*, 38–45.
22. Bazrafshan, E.; Mostafapour, F.K.; Hosseini, A.R.; Khorshid, A.R.; Mahvi, A.H. Decolorisation of reactive red 120 dye by using single-walled carbon nanotubes in aqueous solutions. *J. Chem.* **2013**, *2013*, 938374. [CrossRef]
23. Jawad, A.H.; Mohammed, I.A.; Abdulhameed, A.S. Tuning of fly ash loading into chitosan-ethylene glycol diglycidyl ether composite for enhanced removal of reactive red 120 dye: Optimization using the Box–Behnken design. *J. Polym. Environ.* **2020**, *28*, 2720–2733. [CrossRef]
24. Khanam, A.; Nadeem, F.; Praveena, S.M.; Rashid, U. Removal of dyes using alginated, calcinized and hybrid materials–A comprehensive review. *Int. J. Chem. Biochem. Sci.* **2017**, *12*, 130–140.
25. Noreen, S.; Bhatti, H.N.; Zuber, M.; Zahid, M.; Asgher, M. Removal of actacid orange-RL dye using biocomposites: Modeling studies. *Pol. J. Environ. Stud.* **2017**, *26*, 2125–2134. [CrossRef]
26. Amin, N.K. Removal of direct blue-106 dye from aqueous solution using new activated carbons developed from pomegranate peel: Adsorption equilibrium and kinetics. *J. Hazard. Mater.* **2009**, *165*, 52–62. [CrossRef] [PubMed]
27. Toor, M.; Jin, B. Adsorption characteristics, isotherm, kinetics, and diffusion of modified natural bentonite for removing diazo dye. *Chem. Eng. J.* **2012**, *187*, 79–88. [CrossRef]
28. El-Nagar, D.A.; Sary, D.H. Synthesis and characterization of nano bentonite and its effect on some properties of sandy soils. *Soil Tillage Res.* **2021**, *208*, 104872. [CrossRef]

29. Zaitan, H.; Bianchi, D.; Achak, O.; Chafik, T. A comparative study of the adsorption and desorption of o-xylene onto bentonite clay and alumina. *J. Hazard. Mater.* **2008**, *153*, 852–859. [CrossRef]
30. Saeed, A.; Hanif, M.A.; Nawaz, H.; Qadri, R.W.K. The production of biodiesel from plum waste oil using nano-structured catalyst loaded into supports. *Sci. Rep.* **2021**, *11*, 24120. [CrossRef]